

# Channel state information estimation for 5G wireless communication systems: Recurrent neural networks approach

Mohamed Hassan Ali <sup>Corresp., 1</sup>, Ibrahim B. M. Taha <sup>2</sup>

<sup>1</sup> Department of Electrical Engineering, Faculty of Engineering, Al-Azhar University,, 1Department of Electrical Engineering, Faculty of Engineering, Al-Azhar University, Qena 83513, Egypt, Qena, Qena, Egypt

<sup>2</sup> Department of Electrical Engineering, College of Engineering,, Taif University, Taif 21944,, Saudi Arabia, Taif, Taif

Corresponding Author: Mohamed Hassan Ali  
Email address: mhessai@azhar.edu.eg

In this study, a deep learning bidirectional long short-term memory (BiLSTM) recurrent neural network-based channel state information estimator is proposed for 5G orthogonal frequency-division multiplexing systems. The proposed estimator is a pilot-dependent estimator and follows the online learning approach in the training phase and the offline approach in the practical implementation phase. The estimator does not deal with complete a priori certainty for channels' statistics and attains superior performance in the presence of a limited number of pilots. A comparative study is conducted using three loss functions, namely, mean absolute error, cross entropy function for  $k$ th mutually exclusive classes and sum of squared of the errors. The Adam optimisation algorithm is used to evaluate the performance of the proposed estimator under each loss function. In terms of symbol error rate and accuracy metrics, the proposed estimator outperforms long short-term memory (LSTM) neural network-based channel state information, least squares and minimum mean square error estimators under different simulation conditions. The computational and training time complexities for deep learning BiLSTM- and LSTM-based estimators are provided. Given that the proposed estimator relies on the deep learning neural network approach, where it can analyse massive data, recognise statistical dependencies and characteristics, develop relationships between features and generalise the accrued knowledge for new datasets that it has not seen before, the approach is promising for any 5G and beyond communication system.

# 1 Channel State Information Estimation for 5G Wireless 2 Communication Systems: Recurrent Neural Networks 3 Approach

4  
5

6 Mohamed Hassan Essai Ali<sup>1</sup> and Ibrahim B. M. Taha<sup>2</sup>

7  
8

9 <sup>1</sup>Department of Electrical Engineering, Faculty of Engineering, Al-Azhar University, Qena  
10 83513, Egypt

11 <sup>2</sup>Department of Electrical Engineering, College of Engineering, Taif University, Taif 21944,  
12 Saudi Arabia

13  
14

15 Corresponding Author:

16 Mohamed Hassan Essai Ali <sup>1</sup>

17 Masaken Osman, Qena, Qena, 83513, Egypt

18 Email address: mhessai@azhar.edu.eg

19  
20

## 20 Abstract

21 In this study, a deep learning bidirectional long short-term memory (BiLSTM) recurrent neural  
22 network-based channel state information estimator is proposed for 5G orthogonal frequency-  
23 division multiplexing systems. The proposed estimator is a pilot-dependent estimator and follows  
24 the online learning approach in the training phase and the offline approach in the practical  
25 implementation phase. The estimator does not deal with complete a priori certainty for channels'  
26 statistics and attains superior performance in the presence of a limited number of pilots. A  
27 comparative study is conducted using three loss functions, namely, mean absolute error, cross  
28 entropy function for kth mutually exclusive classes and sum of squared of the errors. The Adam  
29 optimisation algorithm is used to evaluate the performance of the proposed estimator under each  
30 loss function. In terms of symbol error rate and accuracy metrics, the proposed estimator  
31 outperforms long short-term memory (LSTM) neural network-based channel state information,  
32 least squares and minimum mean square error estimators under different simulation conditions.  
33 The computational and training time complexities for deep learning BiLSTM- and LSTM-based  
34 estimators are provided. Given that the proposed estimator relies on the deep learning neural  
35 network approach, where it can analyse massive data, recognise statistical dependencies and  
36 characteristics, develop relationships between features and generalise the accrued knowledge for  
37 new datasets that it has not seen before, the approach is promising for any 5G and beyond  
38 communication system.

39

## 40 Introduction

41 5G wireless communication is the most active area of technology development and a rapidly  
42 growing branch of the wider field of communication systems. Wireless communication has made  
43 various possible services ranging from voice to multimedia.

44 The physical characteristics of the wireless communication channel and many unknown  
45 surrounding effects result in imperfections in the transmitted signals. For example, the  
46 transmitted signals experience reflections, diffractions, and scattering, which produce multipath  
47 signals with different delays, phase shift, attenuation, and distortion arriving at the receiving end;  
48 hence, they adversely affect the recovered signals (Oyerinde & Mneney 2012b).

49 A priori information on the physical characteristics of the channel provided by pilots is one of  
50 the significant factors that determine the efficiency of channel state information estimators  
51 (CSIEs). For instance, if not a priori information is available (no or insufficient pilots), channel  
52 estimation is useless; finding what you do not know is impossible. When complete information  
53 on the transmission channel is available, CSIEs are no longer needed. Thus, a priori uncertainty  
54 exists for communication channel statistics. However, the classical theory of detection,  
55 recognition, and estimation of signals deals with complete priory certainty for channel statistics,  
56 and it is an unreliable and unpractical assumption (Bogdanovich et al. 2009).

57 In the classic case, uncertainty is related to useful signals. In detection problems, the unknown  
58 is the fact of a signal existence. In recognition problems, the unknown is the type of signal being  
59 received at the current moment. In estimation problems, the unknown is the amplitude of the  
60 measured signal or one of its parameters. The rest of the components of the signal-noise  
61 environment in classical theory are regarded as a priori certain (known) as follows: the known is  
62 the statistical description of the noise, the known is the values of the unmeasured parameters of  
63 the signal and the known is the physical characteristics of the wireless communication channel.  
64 In such conditions, the classical theory allows the synthesis of optimal estimation algorithms, but  
65 the structure and quality coefficients of the algorithms depend on the values of the parameters of  
66 the signal-noise environment. If the values of the parameters describing the signal-noise  
67 environment are slightly different from the parameters for which the optimal algorithm is built,  
68 then the quality coefficients will become substantially poor, making the algorithm useless in  
69 several cases (Bogdanovich et al. 2009), (O'Shea et al. 2017). The most frequently used CSIEs  
70 are derived from signal and channel statistical models by employing techniques, such as  
71 maximum likelihood (ML), least squares (LS), and minimum mean squared error (MMSE)  
72 optimisation metrics (Kim 2015).

73 One of the major concerns in the optimum performance of wireless communication systems is  
74 providing accurate channel state information (CSI) at the receiver end of the systems to detect  
75 the transmitted signal coherently. If CSI is unavailable at the receiver end, then the transmitted  
76 signal can only be demodulated and detected by a noncoherent technique, such as differential  
77 demodulation. However, using a noncoherent detection method occurs at the expense of a loss of  
78 signal-to-noise ratio of about 3–4 dB compared with using a coherent detection technique. To  
79 eliminate such losses, researchers have focused on the development of channel estimation  
80 techniques to provide perfect detection of transmitted information in wireless communication  
81 systems using the Orthogonal Frequency-Division Multiplexing (OFDM) modulation scheme  
82 (Oyerinde & Mneney 2012a).

83 The use of deep learning neural networks (DLNNs) is the state-of-the-art approach in the field  
84 of wireless communication. The amazing learning capabilities of DLNNs from training data sets  
85 and the tremendous progress of graphical processing units (GPUs), which are considered the  
86 most powerful tools for training DLNNs, have motivated its usage for different wireless  
87 communication issues, such as modulation recognition (Zhou et al. 2020), (Karra et al. 2017) and  
88 channel state estimation and detection (Essai Ali ; Joo et al. 2019; Kang et al. 2020; Ma et al.  
89 2018; Ponnaluru & Penke 2020; Yang et al. 2019a; Ye et al. 2018). According to (Karra et al.  
90 2017; Kim 2015; Oyerinde & Mneney 2012a; Zhou et al. 2020) and (Ma et al. 2018), all  
91 proposed deep learning-based CSIEs have better performance compared with the examined  
92 traditional channel ones, such as LS and MMSE estimators.

93 Recently, numerous long short-term memory (LSTM)- and BiLSTM-based applications have  
94 been introduced for prognostic and health management (Zhao et al. 2020), artificial intelligence-  
95 based translation systems (Wu et al. 2016), (Ong 2017) and other areas. For channel state  
96 information estimation in 5G-OFDM wireless communication systems, many deep learning  
97 approaches, such as convolutional neural network (CNN), recurrent neural network (RNN) (e.g.  
98 LSTM and BiLSTM NNs) and hybrid (CNN and RNN) neural networks have been used (Essai  
99 Ali ; Liao et al. 2019; Luo et al. 2018a; Ponnaluru & Penke 2020; Yang et al. 2019a; Yang et al.  
100 2019b; Ye et al. 2018).

101 In (Liao et al. 2019), a deep learning-based CSIE was proposed by using CNN and BiLSTM-  
102 NN for the extraction of the feature vectors of the channel response and channel estimation,  
103 respectively. The aim was to improve the channel state information estimation performance at  
104 the downlink, which is caused by the fast time-varying and varying channel statistical  
105 characteristics in high-speed mobility scenarios. In (Luo et al. 2018b), an online-trained CSIE  
106 that is an integration of CNN and LSTM-NN was proposed. The authors also developed an  
107 offline–online training technique that applies to 5G wireless communication systems. In (Ye et  
108 al. 2018), a joint channel estimator and detector that is based on feedforward DLNNs for  
109 frequency selective channel (OFDM) systems was introduced. The proposed algorithm was  
110 found to be superior to the traditional MMSE estimation method when unknown surrounding  
111 effects of communication systems are considered. In (Yang et al. 2019b), an online estimator  
112 was developed by adopting feedforward DLNNs for doubly selective channels. The proposed  
113 estimator was considered superior to the traditional LMMSE estimator in all investigated  
114 scenarios. In (Ponnaluru & Penke 2020), a one-dimensional CNN (1D-CNN) deep learning  
115 estimator was proposed. Under various modulation scenarios and in terms of MSE and BER  
116 metrics, the authors compared the performance of the proposed estimator with that of  
117 feedforward neural networks (FFNN), MMSE and LS estimators. 1D-CNN outperformed LS,  
118 MMSE and FFNN estimators. In (Essai Ali), an online pilot-assisted estimator model for OFDM  
119 wireless communication systems was developed by using LSTM NN. The conducted  
120 comparative study showed the superior performance of the proposed estimator in comparison  
121 with LS and MMSE estimators under limited pilots and a prior uncertainty of channel statistics.  
122 The authors in (Sarwar et al. 2020) used the genetic algorithm-optimised artificial neural network  
123 to build a CSIE. The proposed estimator was dedicated for space–time block-coding MIMO-  
124 OFDM communication systems. The proposed estimator outperformed LS and MMSE  
125 estimators in terms of BER at high SNRs, but it achieved approximately the same performance  
126 as LS and MMSE estimators at low SNRs. The authors in (Senol et al. 2021) proposed a CSIE  
127 for OFDM systems by using ANN under the condition of sparse multipath channels. The  
128 proposed estimator achieved a comparable SER performance as matching pursuit- and  
129 orthogonal matching pursuit-based estimators at a lower computational complexity than that of  
130 the examined estimators. The authors in (Le Ha et al. 2021) proposed a CSIE that uses deep  
131 learning and LS estimator and utilizes the multiple-input multiple-output system for 5G-OFDM.  
132 The proposed estimator minimizes the MSE loss function between the LS-based channel  
133 estimation and the actual channel. The proposed estimator outperformed LS and LMMSE  
134 estimators in terms of BER and MSE metrics.

135 In this study, a BiLSTM DLNN-based CSIE for OFDM wireless communication systems is  
136 proposed and implemented. To the best of the authors' knowledge, this work is the first to use  
137 the BiLSTM network as a CSIE without integration with CNN. The proposed estimator does not  
138 need any prior knowledge of the communication channel statistics and powerfully works at  
139 limited pilots (under the condition of less CSI). The proposed BiLSTM-based CSIE is a data-  
140 driven estimator, so it can analyse, recognise and understand the statistical characteristics of  
141 wireless channels suffering from many known interferences such as adjacent channel, inter  
142 symbol, inter user, inter cell, co-channel and electromagnetic interferences and unknown ones  
143 (Jeya et al. 2019; Sheikh 2004). Although an impressively wide range of configurations can be  
144 found for almost every aspect of deep neural networks, the choice of loss function is  
145 underrepresented when addressing communication problems, and most studies and applications  
146 simply use the 'log' loss function (Janocha & Czarnecki 2017). In this study two customized loss

147 functions known as mean absolute error (MAE), and sum of squared errors (SSE) are proposed  
 148 to obtain the most reliable and robust estimator under unknown channel statistical characteristics  
 149 and limited pilot numbers.

150 The performance of the proposed BiLSTM-based estimator is compared with the performance  
 151 of the most frequently used LS and MMSE channel state estimators. The obtained results show  
 152 that the BiLSTM-based estimator attains a comparable performance as the MMSE estimator and  
 153 outperforms LS and MMSE estimators at large and small numbers of pilots, respectively. In  
 154 addition, the proposed estimator improves the transmission data rate of OFDM wireless  
 155 communication systems because it exhibits optimal performance compared with the examined  
 156 estimators at a small number of pilots.

157 The rest of this paper is organised as follows. The DLNN-based CSIE is presented in Section  
 158 II. The standard OFDM system and the proposed deep learning BiLSTM NN-based CSIE are  
 159 presented in Section III. The simulation results are given in Section IV. The conclusions and  
 160 future work directions are provided in Section V.

161

## 162 DLNN-BASED CSIE

163 In this section, a deep learning BiLSTM NN for channel state information estimation is  
 164 presented. The BiLSTM network is another version of LSTM neural networks, which are  
 165 recurrent neural networks (RNN) that can learn the long-term dependencies between the time  
 166 steps of input data (Hochreiter & Schmidhuber 1997) (Luo et al. 2018a; Zhao et al. 2020).

167 The BiLSTM architecture mainly consists of two separate LSTM-NNs and has two  
 168 propagation directions (forward and backward). The LSTM NN structure consists of input,  
 169 output and forget gates and a memory cell. The forget and input gates enable the LSTM NN to  
 170 effectively store long-term memory. Figure 1 shows the main construction of the LSTM cell  
 171 (Hochreiter & Schmidhuber 1997). The forget gate enables LSTM NN to remove the undesired  
 172 information by currently used input  $x_t$  and cell output  $h_t$  of the last process. The input gate finds  
 173 the information that will be used with the previous LSTM cell state  $c_{t-1}$  to obtain a new cell state  
 174  $c_t$  based on the current cell input  $x_t$  and the previous cell output  $h_{t-1}$ . Using the forget and input  
 175 gates, LSTM can decide which information is abandoned and which is retained.

176 The output gate finds current cell output  $h_t$  by using the previous cell output  $h_{t-1}$  at current cell  
 177 state  $c_t$  and input  $x_t$ . The mathematical model of the LSTMNN structure can be described  
 178 through Equations (1) – (6).

$$179 \quad i_t = \sigma_g (w_i x_t + R_i h_{t-1} + b_i), \quad (1)$$

$$180 \quad f_t = \sigma_g (w_f x_t + R_f h_{t-1} + b_f), \quad (2)$$

$$181 \quad g_t = \sigma_c (w_g x_t + R_g h_{t-1} + b_g), \quad (3)$$

$$182 \quad o_t = \sigma_g (w_o x_t + R_o h_{t-1} + b_o), \quad (4)$$

$$183 \quad c_t = f_t \odot c_{t-1} + i_t \odot g_t, \quad (5)$$

$$184 \quad h_t = o_t \odot \sigma_c(c_t), \quad (6)$$

185 where  $i, f, g, o, \sigma_c, \sigma_g$  and  $\odot$  denote the input gate, forget gate, cell candidate, output gate, state  
 186 activation function (hyperbolic tangent function (tanh), gate activation function (sigmoid  
 187 function) and Hadamard product (element-wise multiplication of vectors), respectively.

188  $\mathbf{W} = [w_i \ w_f \ w_g \ w_o]^T$ ,  $\mathbf{R} = [R_i \ R_f \ R_g \ R_o]^T$  and  $\mathbf{b} = [b_i \ b_f \ b_g \ b_o]^T$  are input weights, recurrent weights  
 189 and bias, respectively.

190 The forward and backward propagation directions of BiLSTM are transmitted at the same time  
 191 to the output unit. Therefore, old and future information can be captured, as shown in Figure 2.  
 192 At any time  $t$ , the input is fed to forward LSTM and backward LSTM networks. The final output  
 193 of BiLSTM-NN can be expressed as follows:

$$194 \quad h_t = \vec{h}_t \odot \overleftarrow{h}_t, \quad (7)$$

195 where  $\vec{h}_t$  and  $\overleftarrow{h}_t$  are forward and backward outputs of BiLSTM-NN, respectively.

196 As the proposed BiLSTM-based CSIE is built, the weights and biases of the proposed  
 197 estimator are optimised (tuned) using the Adam optimization algorithm. Adam trains the  
 198 proposed estimator by using one of three loss functions, namely, cross entropy function for  $k^{\text{th}}$   
 199 mutually exclusive classes (crossentropyex), mean absolute error (MAE), and sum of squared  
 200 errors (SSE). The loss function estimates the loss between the expected and actual outcome.  
 201 During the learning process, optimisation algorithms try to minimise the available loss function  
 202 to the desired error goal by optimising the DLNN weights and biases iteratively at each training  
 203 epoch. Selecting a loss function is one of the essential and challenging tasks in deep learning.  
 204 The proposed estimator is trained using above-mentioned three different loss functions to obtain  
 205 the most optimal BiLSTM-based estimator for wireless communication systems with low prior  
 206 information (limited pilots) for signal-noise environments.

207  
 208 To build the DL BiLSTM NN-based CSIE, an array is created with the following five layers:  
 209 sequence input, BiLSTM, fully connected, softmax and output classification. The input size was  
 210 set to 256. The BiLSTM layer consists of 16 hidden units and shows the sequence's last element.  
 211 Four classes are specified by considering the size 4 fully connected (FC) layer, followed by a  
 212 softmax layer and ended by a classification layer. Figure 3 illustrates the structure of the  
 213 proposed estimator (Essai Ali).

214

215

## 216 DL BiLSTM NN-BASED CSIE for 5G-OFDM WIRELESS

### 217 COMMUNICATION SYSTEMS

218 The standard OFDM wireless communication system and an offline DL of the proposed CSIE  
 219 are presented in the following subsections.

220

### 221 OFDM SYSTEM MODEL

222 In accordance with (Essai Ali ; Ye et al. 2018), Figure 4 clearly illustrates the structure of the  
 223 traditional OFDM communication system. On the transmitter side, a serial-to-parallel (S/P)  
 224 converter is used to convert the transmitted symbols with pilot signals into parallel data streams.  
 225 Then, inverse discrete Fourier transform (IDFT) is applied to convert the signal into the time  
 226 domain. A cyclic prefix (CP) must be added to alleviate the effects of inter-symbol interference.  
 227 The length of the CP must be longer than the maximum spreading delay of the channel.

228 The multipath channel of a sample space defined by complex random variables  $\{h(n)\}_{n=0}^{N-1}$   
 229  $\{h(n)\}_{n=0}^{N-1}$  is considered. Then, the received signal can be evaluated as follows:

$$230 \quad y(n) = x(n) \oplus h(n) + w(n) \quad y(n) = x(n) \oplus h(n) + w(n), \quad (8)$$

231 where  $\oplus$   $x(n)$   $x(n)$  is the input signal,  $\oplus$  is circular convolution,  $w(n)$   $w(n)$  is additive white  
 232 Gaussian noise (AWGN) and  $y(n)$   $y(n)$  is the output signal.

233 The received signal in the frequency domain can be defined as

$$234 \quad Y(k) = X(k)H(k) + W(k), Y(k) = X(k)H(k) + W(k) \quad (9)$$

235 where the discrete Fourier transformations (DFT) of  $x(n)$   $x(n)$ ,  $h(n)$   $h(n)$ ,  $y(n)$  and  $w(n)$   $w(n)$  are  
 236  $X(k)$   $X(k)$ ,  $H(k)$   $H(k)$ ,  $Y(k)$   $Y(k)$  and  $W(k)$ ,  $W(k)$  respectively. These discrete Fourier  
 237 transformations are estimated after removing CP.

238 The OFDM frame includes the pilot symbols of the 1<sup>st</sup> OFDM block and the transmitted data of  
 239 the next OFDM blocks. The channel can be considered stationary during a certain frame, but it can  
 240 change between different frames. The proposed DL BiLSTM NN-based CSIE receives the arrived  
 241 data at its input terminal and extracts the transmitted data at its output terminal (Essai Ali), (Ye et  
 242 al. 2018).

243

## 244 OFFLINE DL OF THE DL BILSTM NN-BASED CSIE

245 DLNN utilisation is the state-of-the-art approach in the field of wireless communication, but  
 246 DLNNs have high computational complexity and long training time. GPUs are the most  
 247 powerful tools used for training DLNNs (Sharma et al. 2016). Training should be done offline  
 248 due to the long training time of the proposed CSIE and the large number of BILSTM-NN's  
 249 parameters, such as biases and weights, that should be tuned during training. The trained CSIE is  
 250 then used in online implementation to extract the transmitted data (Ye et al. 2018), (Essai Ali).

251 In offline training, the learning dataset is randomly generated for one subcarrier. The  
 252 transmitting end sends OFDM frames to the receiving end through the adopted (simulated)  
 253 channel, where each frame consists of single OFDM pilot symbol and a single OFDM data  
 254 symbol. The received OFDM signal is extracted based on OFDM frames that are subjected to  
 255 different channel imperfections.

256 All classical estimators rely highly on tractable mathematical channel models, which are  
 257 assumed to be linear, stationary and follow Gaussian statistics. However, practical wireless  
 258 communication systems have other imperfections and unknown surrounding effects that cannot  
 259 be tackled well by accurate channel models; therefore, researchers have developed various  
 260 channel models that effectively characterise practical channel statistics. By using these channel  
 261 models, reliable and practical training datasets can be obtained by modelling (Bogdanovich et al.  
 262 2009), (Essai Ali), (2019).

263 In this study, the 3GPP TR38.901-5G channel model developed by (2019) is used to simulate  
 264 the behaviour of a practical wireless channel that can degrade the performance of CSIEs and  
 265 hence, the overall communication system's performance.

266 The proposed estimator is trained via Adam optimisation, which updates the weights and  
 267 biases by minimising a specific loss function. Simply, a loss function is defined as the difference  
 268 between the estimator's responses and the original transmitted data. The loss function can be  
 269 represented by several functions. MATLAB/neural network toolbox allows the user to choose a  
 270 loss function amongst its available list that contains crossentropyex, MSE, sigmoid and softmax.  
 271 In this study, another two custom loss functions (MAE and SSE) are created. The performance of  
 272 the proposed estimator when using three loss functions (i.e. MAE, crossentropyex and SSE) is  
 273 investigated. The loss functions can be expressed as follows:

$$274 \text{crossentropyex} = -\sum_{i=1}^N \sum_{j=1}^c X_{ij}(k) \log(\hat{X}_{ij}(k)), \text{crossentropyex} = -\sum_{i=1}^N \sum_{j=1}^c X_{ij}(k) \log(\hat{X}_{ij}(k))$$

$$275 \text{MAE} = \frac{\sum_{i=1}^N \sum_{j=1}^c |X_{ij}(k) - \hat{X}_{ij}(k)|}{N} \quad (10)$$

$$276 \text{MAE} = \frac{\sum_{i=1}^N \sum_{j=1}^c |X_{ij}(k) - \hat{X}_{ij}(k)|}{N}, \quad (11)$$

$$277 \text{SSE} = \sum_{i=1}^N \sum_{j=1}^c (X_{ij}(k) - \hat{X}_{ij}(k))^2, \text{SSE} = \sum_{i=1}^N \sum_{j=1}^c (X_{ij}(k) - \hat{X}_{ij}(k))^2 \quad (12)$$

278

279 where  $N$  is the sample number,  $c$  is the class number,  $X_{ij}$  is the  $i$ <sup>th</sup> transmitted data sample for  
 280 the  $j$ <sup>th</sup> class and  $\hat{X}_{ij}$  is the DL BiLSTM-based CSIE response for sample  $i$  for class  $j$ .

281 Figure 5 illustrates the processes of generating the training data sets and offline DL to obtain a  
 282 learned CSIE based on BiLSTM-NN.

283

## 284 Simulation Results

### 285 STUDYING THE PERFORMANCE OF THE PROPOSED, LS AND MMSE 286 ESTIMATORS BY USING DIFFERENT PILOTS AND LOSS FUNCTIONS

287 Several simulation experiments are performed to evaluate the performance of the proposed  
 288 estimator. In terms of symbol error rate (SER) performance analysis, the SER performance of the  
 289 proposed estimator under various SNRs is compared with that of the LSTM NN-based CSIE (Essai

290 Ali), the well-known LS estimator and the MMSE estimator, which is an optimal estimator but  
291 requires channel statistical information. A priori uncertainty of the used channel model statistics is  
292 assumed and considered for all conducted experiments.

293 Moreover, the Adam optimisation algorithm is used to train the proposed estimator whilst using  
294 different loss functions to obtain the most robust version of the proposed CSIE. The proposed  
295 model is implemented in 2019b MATLAB/software.

296 Table 1 lists the parameters of BiLSTM-NN and LSTM-NN architectures and their related  
297 training options. These parameters are identified by a trial-and-error approach. Table 2 lists the  
298 parameters of the OFDM system model and the channel model.

299 The examined estimators' performance is evaluated at different pilot numbers of 4, 8 and 64 as  
300 well as crossentropyex, MAE and SSE loss functions. The Adam optimisation algorithm is used  
301 for all simulation experiments.

302 With a sufficiently large number of pilots (64) and the use of the crossentropyex loss function,  
303 the proposed  $\text{BiLSTM}_{\text{crossentropyex}}$  estimator outperforms  $\text{LSTM}_{\text{crossentropyex}}$ , LS and MMSE  
304 estimators over the entire SNR range, as shown in Figure 6. At the use of the MAE loss function,  
305 the  $\text{BiLSTM}_{\text{MAE}}$  estimator outperforms the LS estimator over the SNR range [0–18 dB], but  
306  $\text{LSTM}_{\text{MAE}}$  outperforms it over the SNR range [0–14 dB]. In addition, the  $\text{BiLSTM}_{\text{MAE}}$  and  
307  $\text{LSTM}_{\text{MAE}}$  estimators are at par with the MMSE estimator over the SNR ranges [0–10 dB] and [0–  
308 4 dB], respectively. Beyond these SNR ranges, the MMSE estimator outperforms  $\text{BiLSTM}_{\text{MAE}}$  and  
309  $\text{LSTM}_{\text{MAE}}$  estimators.  $\text{BiLSTM}_{\text{MAE}}$  outperforms  $\text{LSTM}_{\text{MAE}}$  starting from 0 dB to 20 dB.

310 At the use of the SSE loss function, Figure 6 shows that the  $\text{BiLSTM}_{\text{SSE}}$  and  $\text{LSTM}_{\text{SSE}}$   
311 estimators achieve approximately the same performance as the MMSE estimator over a low SNR  
312 range [0–6 dB]. MMSE outperforms the  $\text{BiLSTM}_{\text{SSE}}$  and  $\text{LSTM}_{\text{SSE}}$  estimators starting from 8 dB,  
313 and the LS estimator outperforms  $\text{BiLSTM}_{\text{SSE}}$  starting from 16 dB and  $\text{LSTM}_{\text{SSE}}$  starting from 14  
314 dB.  $\text{BiLSTM}_{\text{SSE}}$  outperforms  $\text{LSTM}_{\text{SSE}}$  starting from 10 dB to 20 dB. LS provides poor  
315 performance compared with MMSE because it does not use prior information about channel  
316 statistics in the estimation process. MMSE exhibits superior performance, especially with  
317 sufficient pilot numbers, because it uses second-order channel statistics. Concisely, MMSE and the  
318 proposed  $\text{BiLSTM}_{\text{crossentropyex}}$  attain close SER performance with respect to all SNRs. Furthermore,  
319 at low SNR (0–6 dB),  $\text{BiLSTM}_{(\text{crossentropyex}, \text{MAE}, \text{and SSE})}$ ,  $\text{LSTM}_{(\text{crossentropyex}, \text{MAE}, \text{and SSE})}$  and MMSE  
320 attain approximately the same performance.

321 Figures 7 present the performance comparison of LS, MMSE, BiLSTM and LSTM-based  
322 estimators using the Adam optimisation algorithm and the different (crossentropyex, MAE and  
323 SSE) loss functions at 8 pilots. Figure 7 shows that the proposed  $\text{BiLSTM}_{(\text{crossentropyex}, \text{or MAE or SSE})}$   
324 estimators outperform the  $\text{LSTM}_{(\text{crossentropyex}, \text{or MAE or SSE})}$  estimators and the traditional estimators  
325 over the examined SNR range. At a low SNR (0–7 dB), the proposed  $\text{BiLSTM}_{(\text{crossentropyex}, \text{or MAE or}$   
326  $\text{SSE})}$  estimators exhibit semi-identical performance. Furthermore, the proposed  $\text{BiLSTM}_{\text{SSE}}$   
327 estimator trained by minimising the SSE loss function outperforms the  $\text{BiLSTM}_{\text{crossentropyex}}$   
328 estimator trained by minimising the crossentropyex loss function starting from 0 dB; also it  
329 outperforms  $\text{BiLSTM}_{\text{MAE}}$ , which is trained by minimising the MAE loss function starting from 14  
330 dB. Concisely at 8 pilots  $\text{BiLSTM}_{\text{SSE}}$  estimator achieved the most minimum SER.

331 Figures 8 show the performance comparison of the LS, MMSE,  $\text{BiLSTM}_{(\text{crossentropyex}, \text{or MAE or}$   
332  $\text{SSE})}$  and  $\text{LSTM}_{(\text{crossentropyex}, \text{or MAE or SSE})}$  estimators at 4 pilots. Figure 8 shows the superiority of the  
333 proposed  $\text{BiLSTM}_{(\text{crossentropyex}, \text{or MAE or SSE})}$  estimators in comparison with the traditional  
334 estimators, which have lost their workability starting from 0 dB. It also shows the superiority of  
335 the proposed estimator  $\text{BiLSTM}_{(\text{MAE or SSE})}$  over  $\text{LSTM}_{(\text{MAE or SSE})}$ .  $\text{LSTM}_{(\text{crossentropyex})}$  exhibits a  
336 competitive performance as  $\text{BiLSTM}_{(\text{crossentropyex})}$  starting from 0 dB to 12 dB, and  
337  $\text{LSTM}_{(\text{crossentropyex})}$  outperforms  $\text{BiLSTM}_{(\text{crossentropyex})}$  starting from 14 dB. At very low SNRs (0–3  
338 dB), the proposed  $\text{BiLSTM}_{(\text{crossentropyex}, \text{or MAE or SSE})}$  estimators have the same performance. The  
339 proposed  $\text{BiLSTM}_{\text{SSE}}$  estimator outperforms the  $\text{BiLSTM}_{\text{crossentropyex}}$  estimator starting from 4 dB,  
340 and it exhibits an identical performance as the  $\text{BiLSTM}_{\text{MAE}}$  estimator until 14 dB and  
341 outperforms it in the rest of the SNR examination range.

342 Figures 6, 7 and 8 emphasise the robustness of the BiLSTM-based estimators against the  
343 limited number of pilots, low SNR, and under the condition of a priori uncertainty of channel

344 statistics. They demonstrate the importance of testing various loss functions in the deep learning  
345 process to obtain the most optimal architecture of any proposed estimator.

346 Figure 9 indicates that the proposed  $\text{BiLSTM}_{\text{crossentropyex}}$ ,  $\text{BiLSTM}_{\text{SSE}}$  and  $\text{BiLSTM}_{\text{SSE}}$   
347 estimators have close SER performance at 64, 8 and 4 pilots, respectively. The performance of  
348  $\text{BiLSTM}_{\text{SSE}}$  at 8 pilots coincides with the performance of  $\text{BiLSTM}_{\text{crossentropyex}}$  at 64 pilots.  
349 Therefore, using the proposed estimators with few pilots is recommended for 5G OFDM wireless  
350 communication systems to attain a significant improvement in their transmission data rate.  
351 Given that the proposed estimator adopts a training data set-driven approach, it is robust to a  
352 priori uncertainty for channel statistics.

353

354

## 355 LOSS CURVES

356 The quality of the DLNNs' training process can be monitored efficiently by exploring the  
357 training loss curves. These loss curves provide information on how the training process goes, and  
358 the user can decide whether to let the training process continue or stop.

359 Figures 10–12 show the loss curves of the DLNN-based estimators ( $\text{BiLSTM}$  and  $\text{LSTM}$ ) at  
360 pilot numbers = 64, 8 and 4 and with the three examined loss functions (crossentropyex, MAE  
361 and SSE). The curves emphasise and verify the obtained results in Figure 6, 7, and 8. For  
362 example, the sub-curves in Figure 10 for  $\text{BiLSTM}_{\text{crossentropyex}}$  and  $\text{LSTM}_{\text{crossentropyex}}$  estimators  
363 emphasise their superiority over the other estimators. This superiority can be seen clearly from  
364 Figures 6. Moreover, the training loss curves in Figures 11 and 12 emphasise the obtained SER  
365 performance in Figures 7 and 8, respectively, of each examined DLNN-based CSIE. For more  
366 details, good zooming, and analysis of the presented loss curves, they can be downloaded from  
367 this link ([shorturl.at/lqxGQ](http://shorturl.at/lqxGQ)).

368

## 369 ACCURACY CALCULATION

370 The accuracy of the proposed and other examined estimators is a measure of how the  
371 estimators recover transmitted data correctly. Accuracy can be defined as the number of correctly  
372 received symbols divided by the total number of transmitted symbols. The proposed estimator is  
373 trained in different conditions as indicated in the previous subsection, and we wish to investigate  
374 how well it performs in a new data set. Tables 3, 4 and 5 present the obtained accuracies for all  
375 examined estimators under all simulation conditions.

376 As illustrated in Tables 3 to 5, the proposed  $\text{BiLSTM}$ -based estimator attains accuracies from  
377 98.61 to 100 under different pilots and loss functions. The other examined DL  $\text{LSTM}$ -based  
378 estimator has accuracies from 97.88 to 99.99 under the same examination conditions. The  
379 achieved accuracies indicate that the proposed estimator has robustly learned and emphasises the  
380 obtained SER performance in Figure 9. The obtained results of MMSE and LS in Tables 1, 2 and  
381 3 emphasise the presented SER performance in Figures 6, 7 and 8, respectively, and show that as  
382 the pilot number decreases, the accuracy of the conventional estimators dramatically decreases.

383 The proposed  $\text{BiLSTM}$ - and  $\text{LSTM}$ -based estimators rely on DLNN approaches, where they  
384 can analyse huge data sets that may be collected from any plant, recognise the statistical  
385 dependencies and characteristics, devise the relationships between features and generalise the  
386 accrued knowledge for new data sets that they have not seen before. Thus, they are applicable to  
387 any 5G and beyond communication system.

388

## 389 COMPLEXITY

390 The feed-forward pass and feed-back pass operations dominate the computational complexity  
391  $O(W)$  of all neural networks, such as FFNNs,  $\text{LSTM}$  and  $\text{BiLSTM}$ . In a feed-forward pass, the  
392 weighted sum of inputs from previous layers to the next layers is calculated. In feed-back pass,  
393 the errors are evaluated; hence, the weights are modified.

394 The computational complexity of  $\text{LSTM}$  is

$$O(W) = O(KH + KCS + HI + CSI), \quad (13)$$

where  $W$  is the weight number,  $K$  is the output unit number,  $H$  is the hidden unit number,  $I$  is the input number,  $C$  is the memory cell block number and  $S$  is the memory cell block size (Hochreiter & Schmidhuber 1997).

The BiLSTM architecture has two separate LSTM-NNs and two propagation directions (forward and backward). Hence, for BiLSTM,  $W = 2W$ . The computational complexity of BiLSTM is

$$O(2W) = O(2(KH + KCS + HI + CSI)). \quad (14)$$

The required training time can be used as another a complexity metric. Table 6 lists the consumed processing time for the examined BiLSTM- and LSTM-based CSIEs. The used computer is equipped with an Intel(R) Core (TM) i5-2400 CPU running with a 3.10–3.30 GHz microprocessor and 4 GB of RAM. The LSTM-based estimators consume less processing time than the BiLSTM-based estimators do. Hence, they have the lowest complexity.

408  
409

## 410 CONCLUSIONS and FUTURE WORK

411 The proposed DL-BiLSTM-based CSIE is an online pilot-assisted estimator. It is robust against a  
412 limited number of pilots and exhibits superior performance compared with conventional  
413 estimators; it is also robust under the conditions of a priori uncertainty of communication channel  
414 statistics (non-Gaussian/stationary statistical channels) and demonstrates superior performance  
415 compared with conventional estimators and DL LSTM NN-based CSIEs.

416 The proposed CSIE exhibits a consistent performance at large and small pilot numbers and  
417 superior performance at low SNRs, especially at limited pilots, compared with conventional  
418 estimators. It also achieves the highest accuracy amongst all examined estimators at 64, 8, and 4  
419 pilots for all the used loss functions.

420 The proposed BiLSTM- and LSTM-based estimators have high prediction accuracies of  
421 98.61% to 100% and 97.88% to 99.99%, respectively, when using crossentropyex, MAE, and  
422 SSE loss functions for 64, 8, and 4 pilots. They are promising for 5G and beyond wireless  
423 communication systems.

424 Two customized loss functions (MAE and SSE) are introduced. The computational and training  
425 time complexities are presented to illustrate the complexity of the proposed estimator compared  
426 with that of the LSTM-based estimator.

427 For future work, authors suggest the following research plans:

- 428 1. Investigating the proposed estimator's performance and accuracy by using other learning  
429 algorithms, such as Adadelta, Adagrad, AMSgrad, AdaMax and Nadam.
- 430 2. Investigating the proposed estimator's performance and accuracy by using different cyclic  
431 prefix lengths and types.
- 432 3. Developing robust loss functions by using robust statistics estimators, such as Tukey, Cauchy,  
433 Huber and Welsh.
- 434 4. Investigating the performance of CNN-, gated recurrent unit (GRU)- and simple recurrent unit  
435 (SRU)-based CSIEs whilst using crossentropyex, MAE and SSE loss functions and for 64, 8  
436 and 4 pilots.

437

## 438 Acknowledgements

439 The authors would like to acknowledge the financial support received from Taif University  
440 Researchers Supporting Project Number (TURSP-2020/61), Taif University, Taif, Saudi Arabia.

441

## 442 References

- 443 2019. 3GPP. TR38.901 Study on Channel Model for Frequencies from 0.5 to 100 GHz; 3GPP:  
444 Sophia Antipolis, France, 2019.
- 445 Bogdanovich V, Vostretsov AJJoCT, and Electronics. 2009. Application of the invariance and  
446 robustness principles in the development of demodulation algorithms for wideband  
447 communications systems. 54:1283-1291.
- 448 Essai Ali MH. Deep learning-based pilot-assisted channel state estimator for OFDM systems.  
449 *IET Communications* 15:257-264. <https://doi.org/10.1049/cmu2.12051>
- 450 Hochreiter S, and Schmidhuber J. 1997. Long Short-Term Memory. 9:1735–1780.  
451 10.1162/neco.1997.9.8.1735
- 452 Janocha K, and Czarnecki WMJapa. 2017. On loss functions for deep neural networks in  
453 classification.
- 454 Jeya R, Amutha B, Nikhilesh N, and Immaculate RRJs. 2019. Signal Interferences in Wireless  
455 Communication-An Overview. 2:3.
- 456 Joo J, Park MC, Han DS, and Pejovic VJIA. 2019. Deep learning-based channel prediction in  
457 realistic vehicular communications. *IEEE Access* 7:27846-27858.
- 458 Kang J-M, Chun C-J, and Kim I-MJIA. 2020. Deep Learning Based Channel Estimation for  
459 MIMO Systems With Received SNR Feedback. *IEEE Access* 8:121162-121181.
- 460 Karra K, Kuzdeba S, and Petersen J. 2017. Modulation recognition using hierarchical deep  
461 neural networks. 2017 IEEE International Symposium on Dynamic Spectrum Access  
462 Networks (DySPAN). p 1-3.
- 463 Kim H. 2015. *Wireless communications systems design*: John Wiley & Sons.
- 464 Le Ha A, Van Chien T, Nguyen TH, and Choi W. 2021. Deep Learning-Aided 5G Channel  
465 Estimation. 2021 15th International Conference on Ubiquitous Information Management  
466 and Communication (IMCOM): IEEE. p 1-7.
- 467 Liao Y, Hua Y, Dai X, Yao H, and Yang X. 2019. ChanEstNet: A deep learning based channel  
468 estimation for high-speed scenarios. ICC 2019-2019 IEEE International Conference on  
469 Communications (ICC): IEEE. p 1-6.
- 470 Luo C, Ji J, Wang Q, Chen X, Li PJIToNS, and Engineering. 2018a. Channel state information  
471 prediction for 5G wireless communications: A deep learning approach.
- 472 Luo C, Ji J, Wang Q, Chen X, Li PJIToNS, and Engineering. 2018b. Channel state information  
473 prediction for 5G wireless communications: A deep learning approach. 7:227-236.
- 474 Ma X, Ye H, and Li Y. 2018. Learning Assisted Estimation for Time- Varying Channels. 2018  
475 15th International Symposium on Wireless Communication Systems (ISWCS). p 1-5.
- 476 O'Shea T, Karra K, and Clancy TC. 2017. Learning approximate neural estimators for wireless  
477 channel state information. 2017 IEEE 27th international workshop on machine learning  
478 for signal processing (MLSP): IEEE. p 1-7.
- 479 Ong T. 2017. Facebook's translations are now powered completely by AI.
- 480 Oyerinde OO, and Mneney SH. 2012a. Review of Channel Estimation for Wireless  
481 Communication Systems. *IETE Technical Review* 29:282-298. 10.4103/0256-  
482 4602.101308
- 483 Oyerinde OO, and Mneney SHJITr. 2012b. Review of channel estimation for wireless  
484 communication systems. *IETE Technical Review* 29:282-298.
- 485 Ponnaluru S, and Penke S. 2020. Deep learning for estimating the channel in orthogonal  
486 frequency division multiplexing systems. *Journal of Ambient Intelligence and Humanized*  
487 *Computing*. 10.1007/s12652-020-02010-1

- 488 Sarwar A, Shah SM, and Zafar I. 2020. Channel Estimation in Space Time Block Coded MIMO-  
489 OFDM System using Genetically Evolved Artificial Neural Network. 2020 17th  
490 International Bhurban Conference on Applied Sciences and Technology (IBCAST):  
491 IEEE. p 703-709.
- 492 Senol H, Tahir ARB, and Özmen AJTS. 2021. Artificial neural network based estimation of  
493 sparse multipath channels in OFDM systems. *Telecommunication Systems*:1-10.
- 494 Sharma R, Vinutha M, and Moharir M. 2016. Revolutionizing machine learning algorithms using  
495 gpus. 2016 International Conference on Computation System and Information  
496 Technology for Sustainable Solutions (CSITSS): IEEE. p 318-323.
- 497 Sheikh AUH. 2004. Interference, Distortion and Noise. *Wireless Communications: Theory and*  
498 *Techniques*. Boston, MA: Springer US, 225-285.
- 499 Wu Y, Schuster M, Chen Z, Le QV, Norouzi M, Macherey W, Krikun M, Cao Y, Gao Q, and  
500 Macherey KJapa. 2016. Google's neural machine translation system: Bridging the gap  
501 between human and machine translation.
- 502 Yang Y, Gao F, Ma X, and Zhang S. 2019a. Deep Learning-Based Channel Estimation for  
503 Doubly Selective Fading Channels. *IEEE Access* 7:36579-36589.  
504 10.1109/ACCESS.2019.2901066
- 505 Yang Y, Gao F, Ma X, and Zhang SJIA. 2019b. Deep learning-based channel estimation for  
506 doubly selective fading channels. 7:36579-36589.
- 507 Ye H, Li GY, and Juang B. 2018. Power of Deep Learning for Channel Estimation and Signal  
508 Detection in OFDM Systems. *IEEE Wireless Communications Letters* 7:114-117.  
509 10.1109/LWC.2017.2757490
- 510 Zhao C, Huang X, Li Y, and Yousaf Iqbal MJS. 2020. A Double-Channel Hybrid Deep Neural  
511 Network Based on CNN and BiLSTM for Remaining Useful Life Prediction. 20:7109.
- 512 Zhou R, Liu F, and Gravelle CW. 2020. Deep Learning for Modulation Recognition: A Survey  
513 With a Demonstration. *IEEE Access* 8:67366-67376. 10.1109/ACCESS.2020.2986330  
514

## Figure 1

Long short-term memory (LSTM) cell.

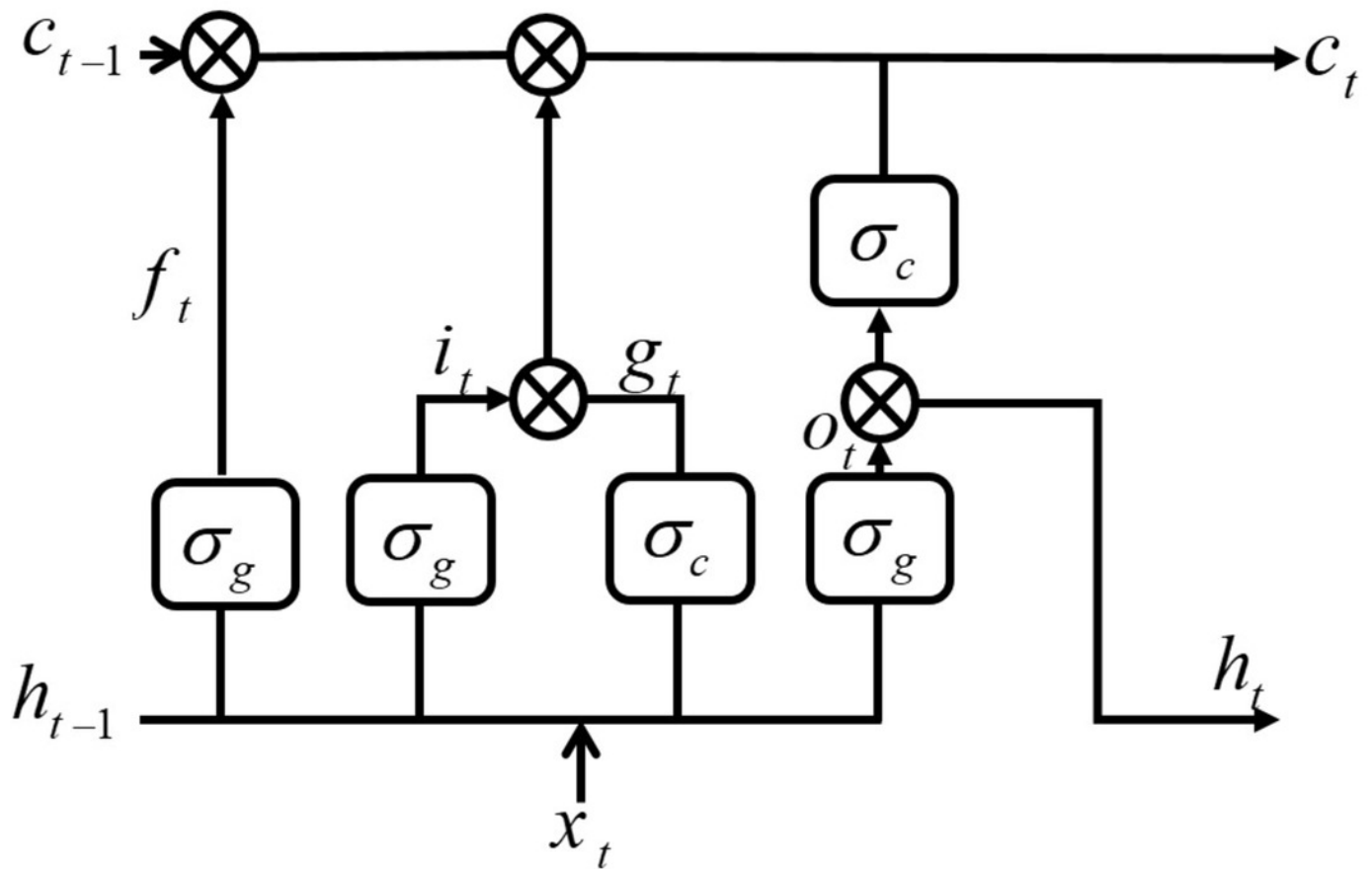


## Figure 2

BiLSTM-NN architecture.

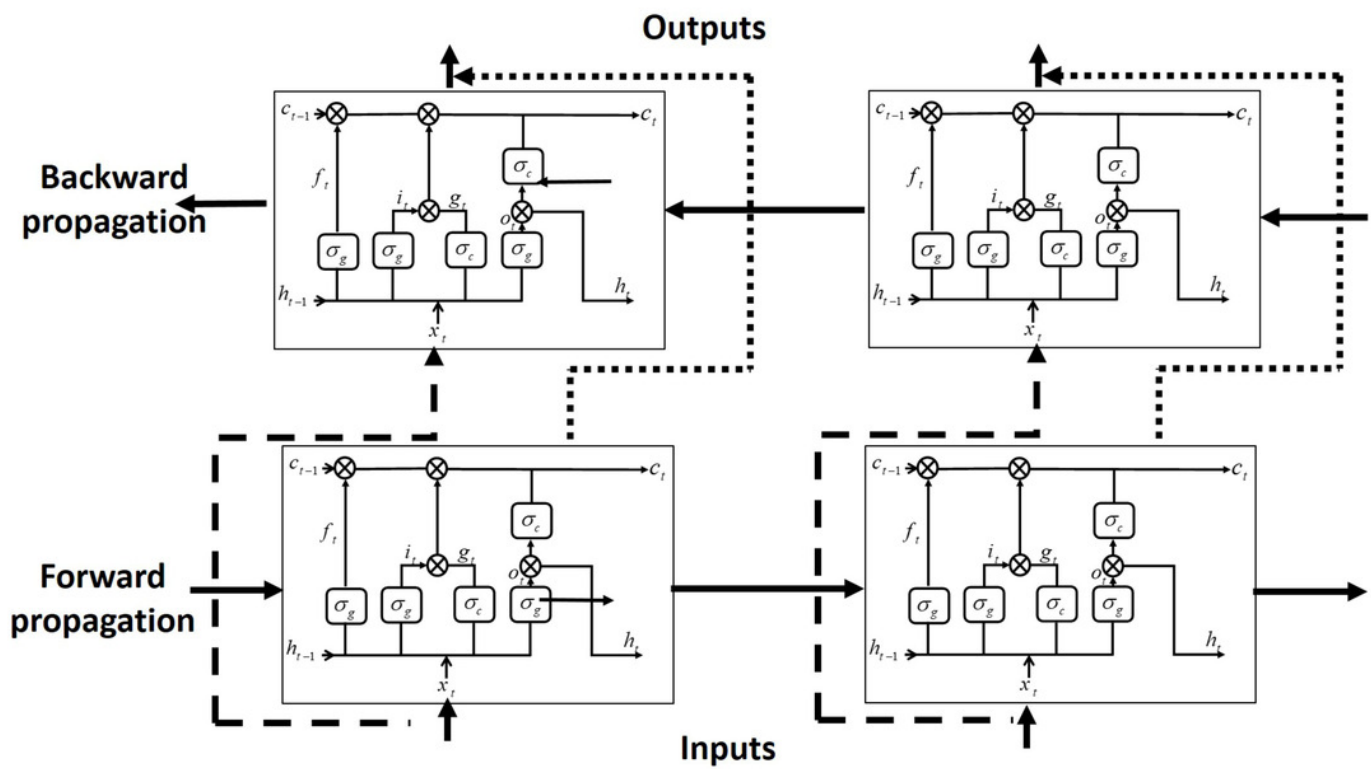


## Figure 3

Structure of the DL BiLSTM NN for the BiLSTM estimator.

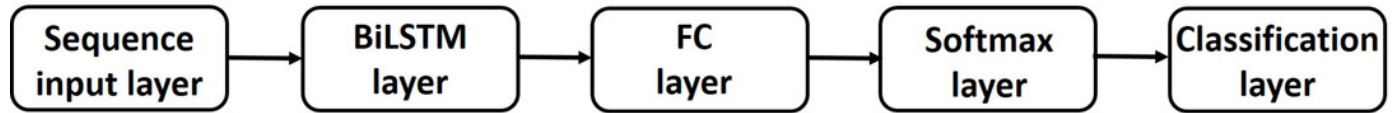


## Figure 4

Conventional OFDM system

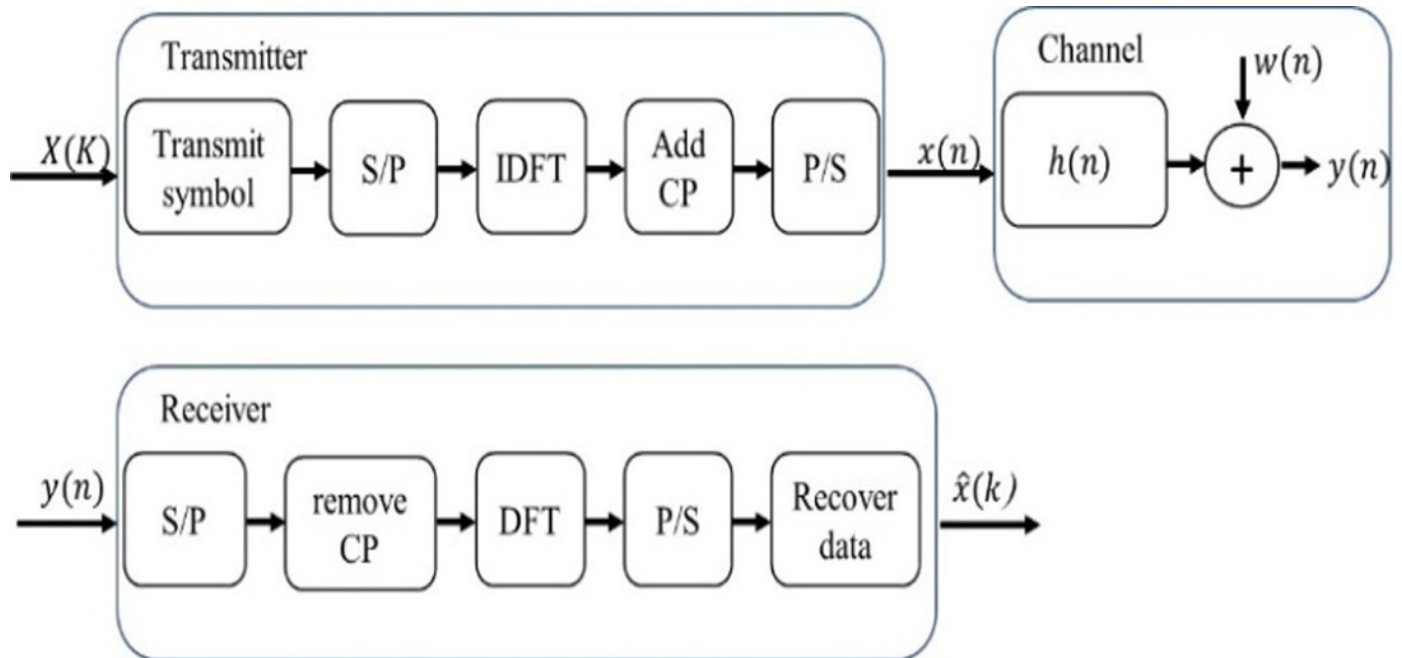


## Figure 5

Training data set formation and offline DL process of the BiLSTM-NN-based CSI estimator.

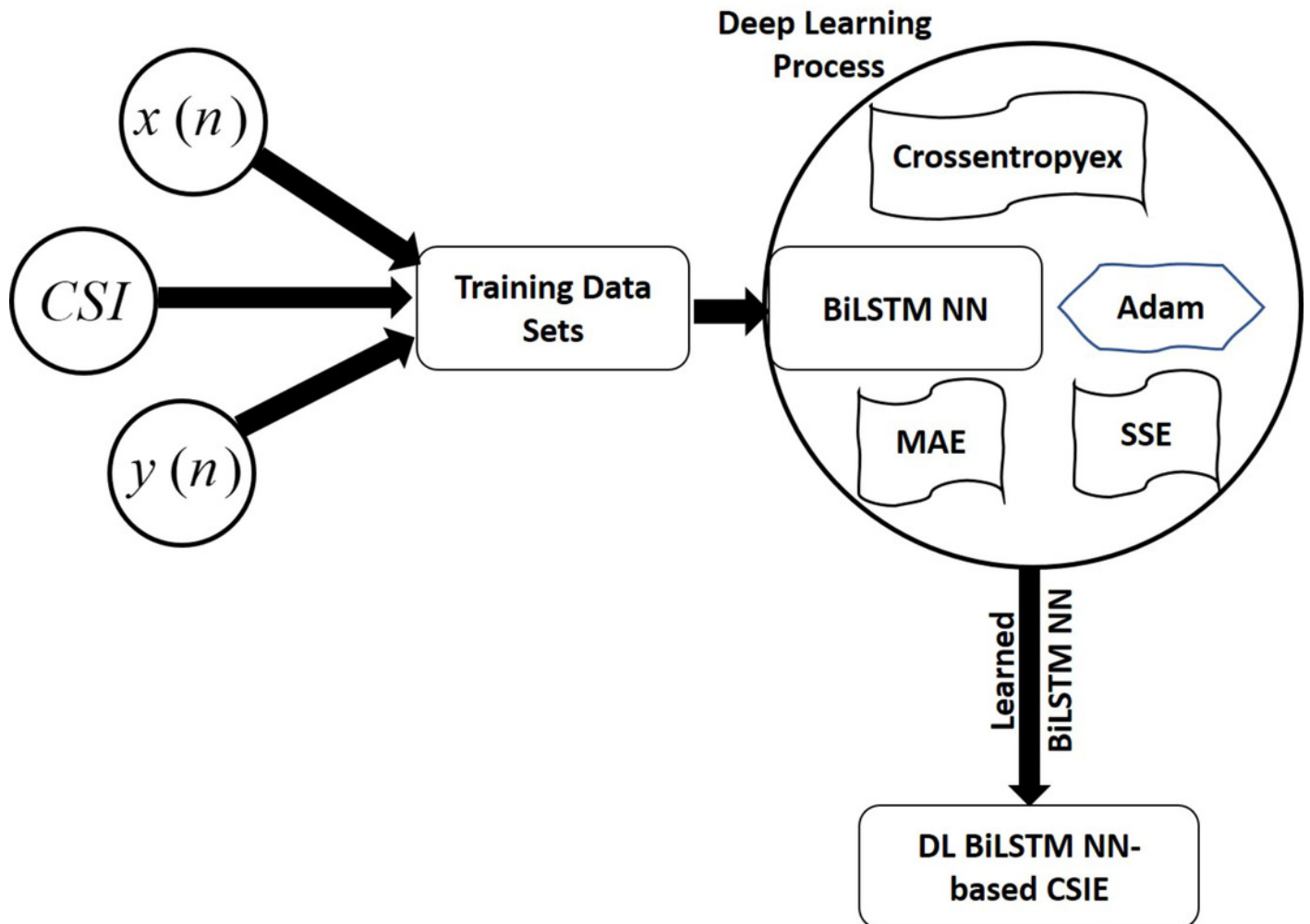


## Figure 6

SER comparison of LS, MMSE, BiLSTM and LSTM estimators using 64 pilots, the Adam learning algorithm and crossentropyex, MAE and SSE loss functions.

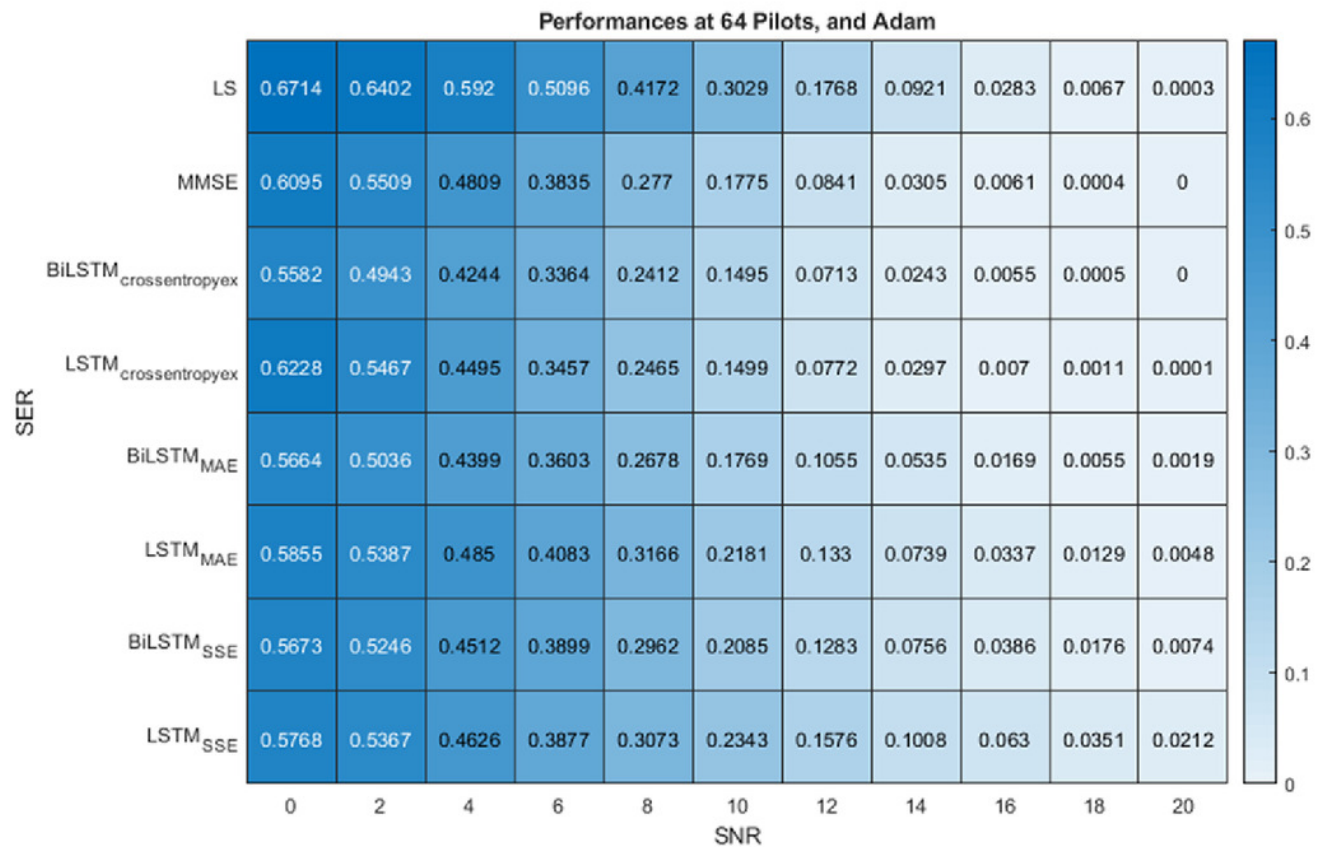


## Figure 7

SER performance comparison of LS, MMSE, BiLSTM, and LSTM estimators using 8 pilots, the Adam learning algorithm and crossentropyex, MAE and SSE loss functions.

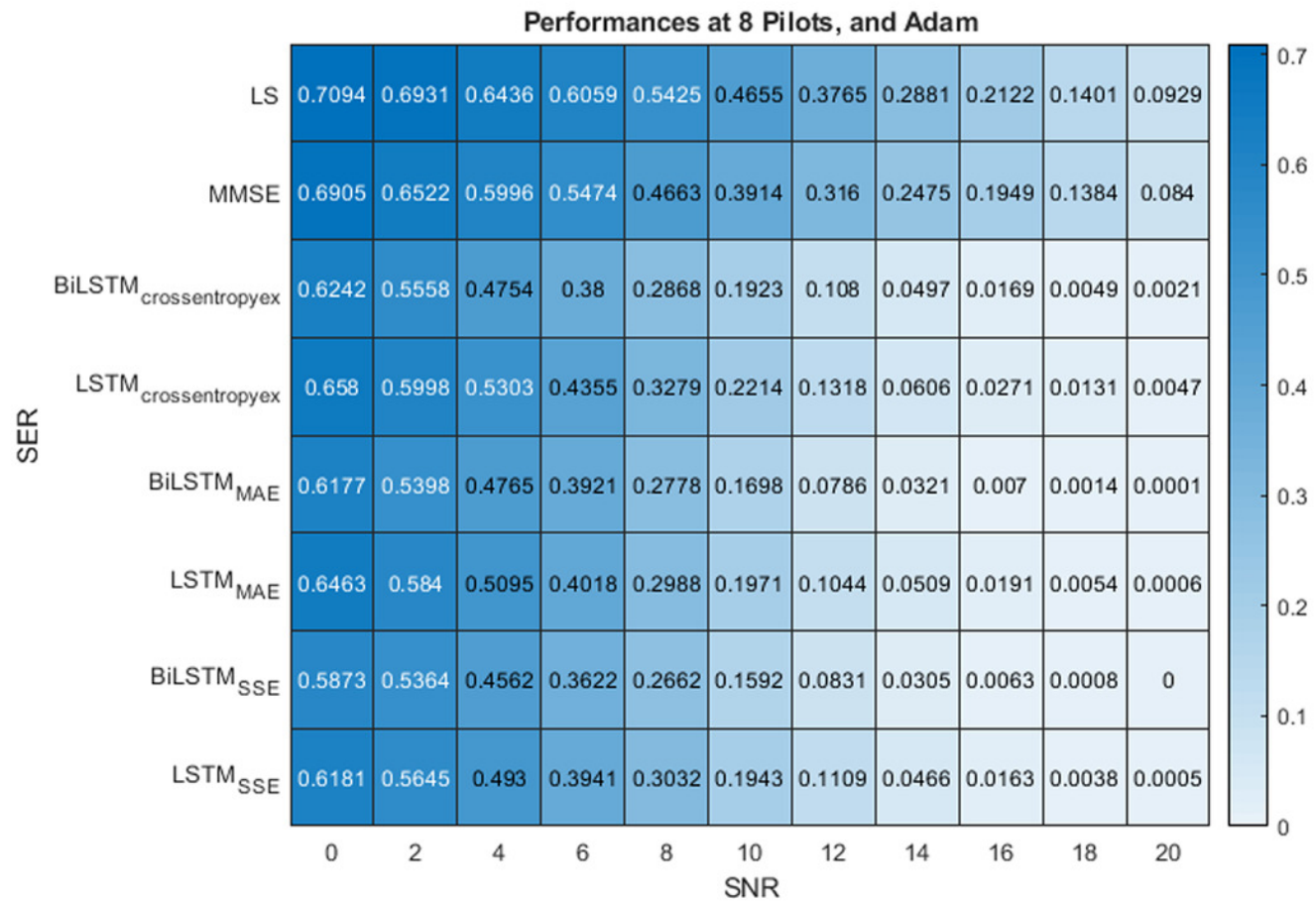


## Figure 8

SER performance comparison of LS, MMSE, BiLSTM, and LSTM estimators using 4 pilots, the Adam learning algorithm and crossentropyex, MAE and SSE loss functions.

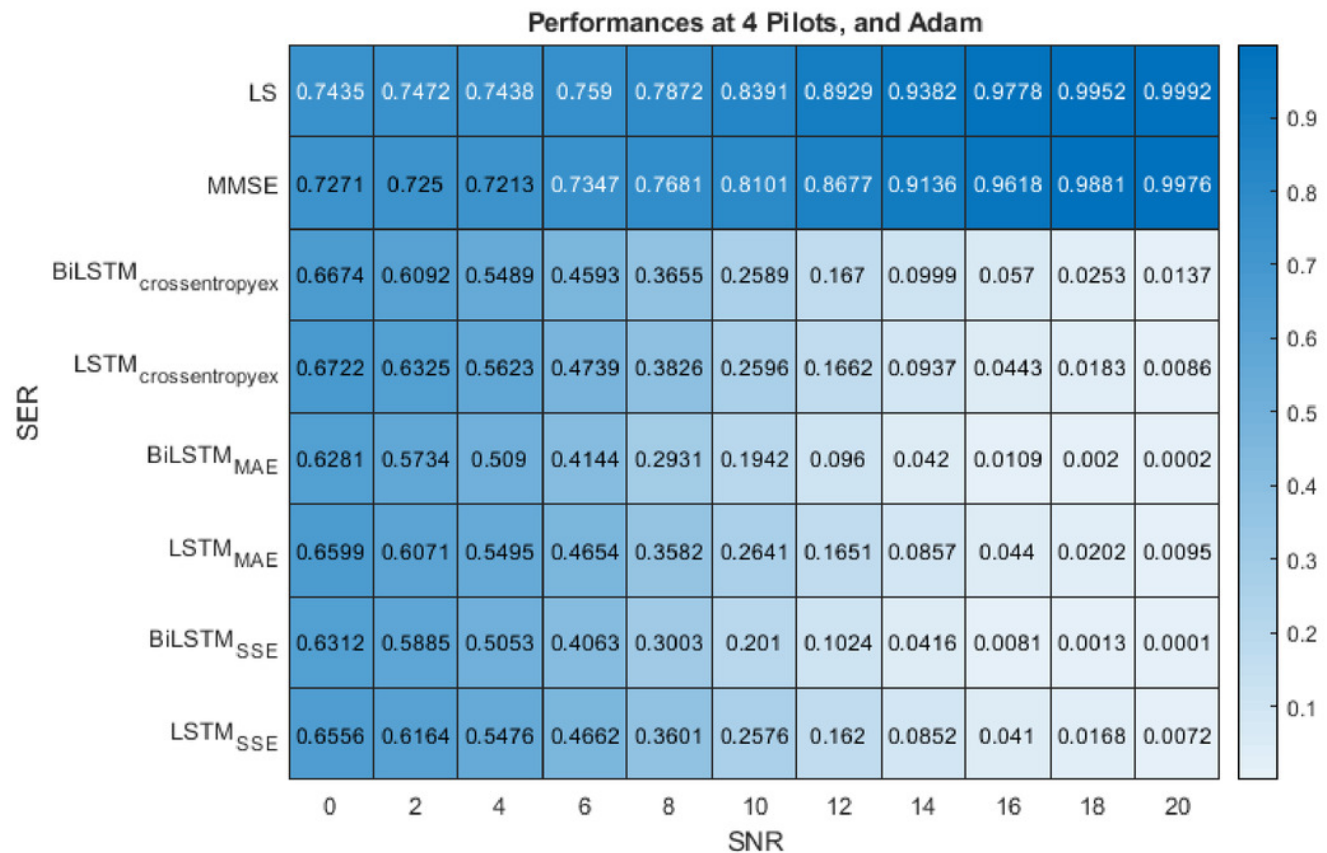


## Figure 9

SER performance comparison of the best DL BiLSTM-based CSIEs using various pilots and loss functions.

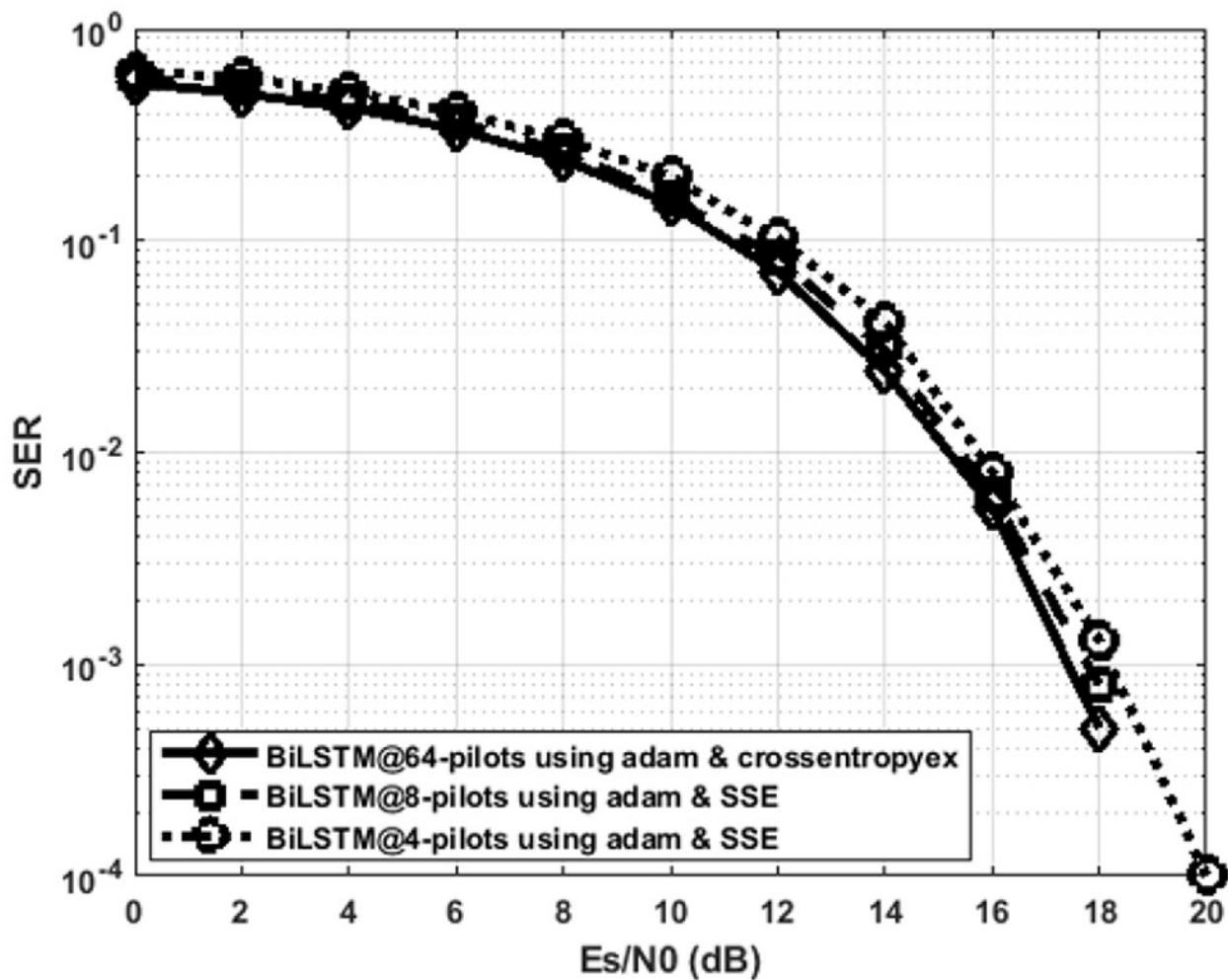


## Figure 10

Loss curves comparison of BiLSTM- and LSTM- based estimators using 64 pilots, the Adam learning algorithm and crossentropyex, MAE and SSE loss functions.

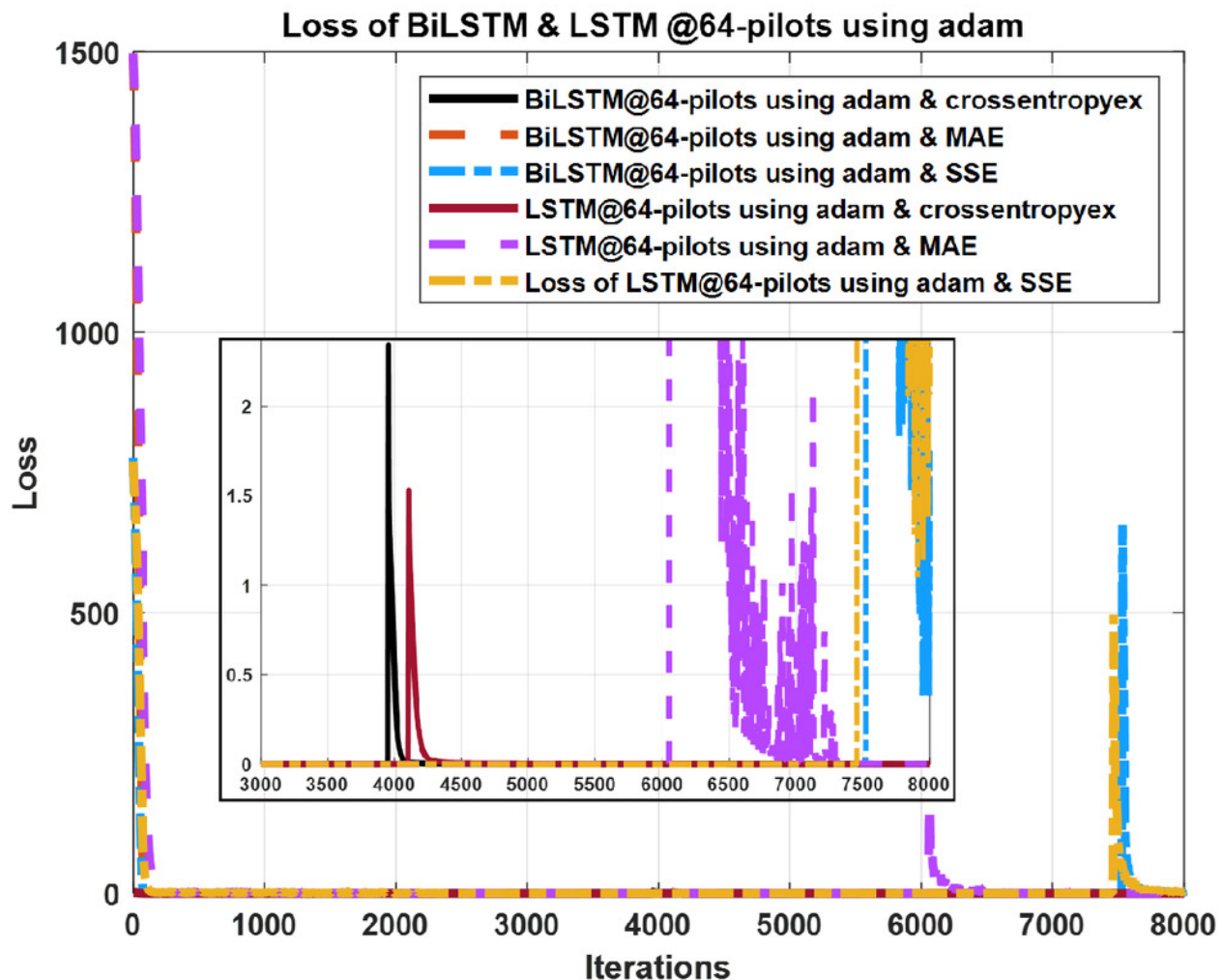


## Figure 11

Loss curves comparison of BiLSTM- and LSTM-based estimators using 8 pilots, the Adam learning algorithm and crossentropyex, MAE and SSE loss functions.

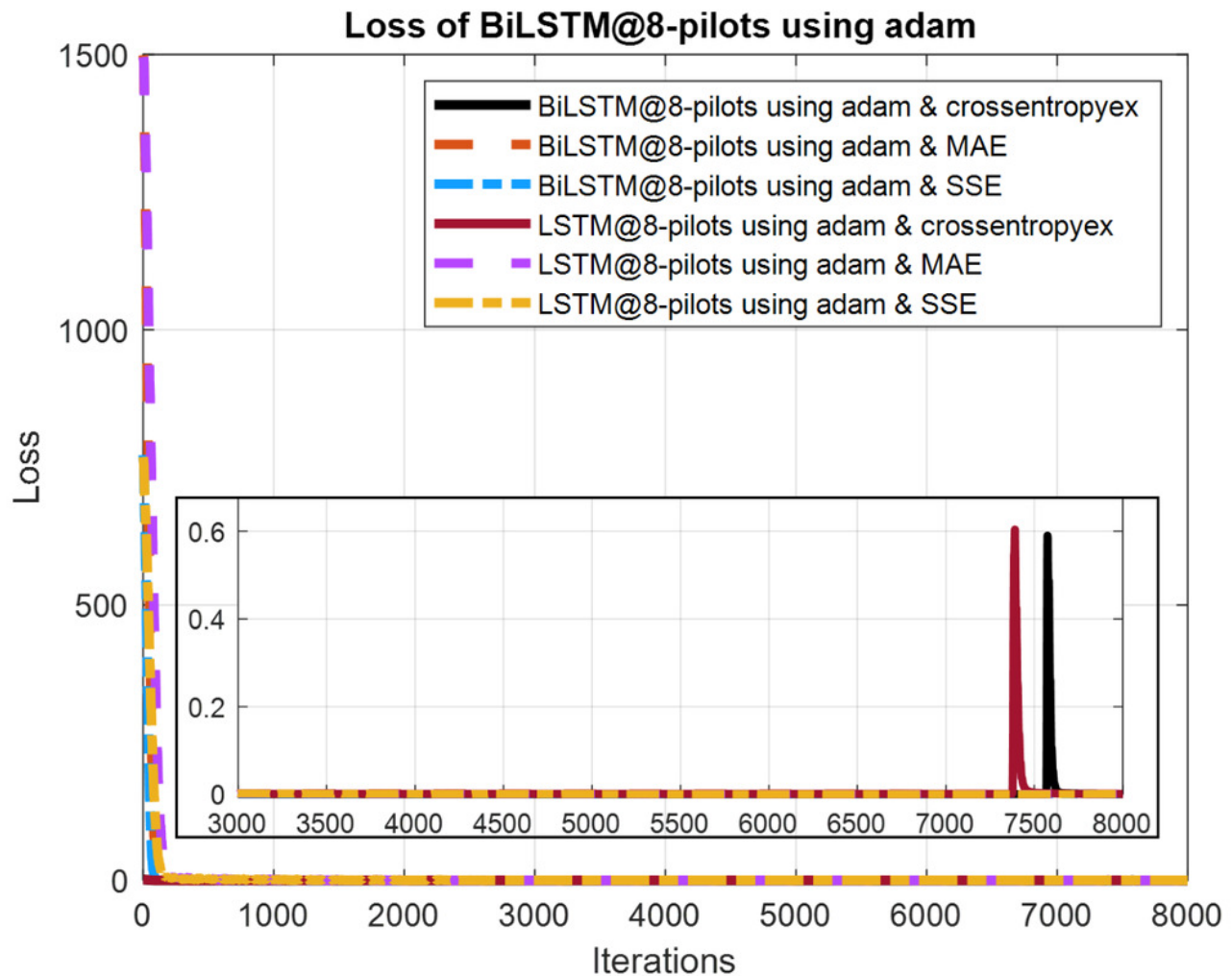


## Figure 12

Loss curves comparison of BiLSTM- and LSTM-based estimators using 4 pilots, the Adam learning algorithm and crossentropy, MAE and SSE loss functions.

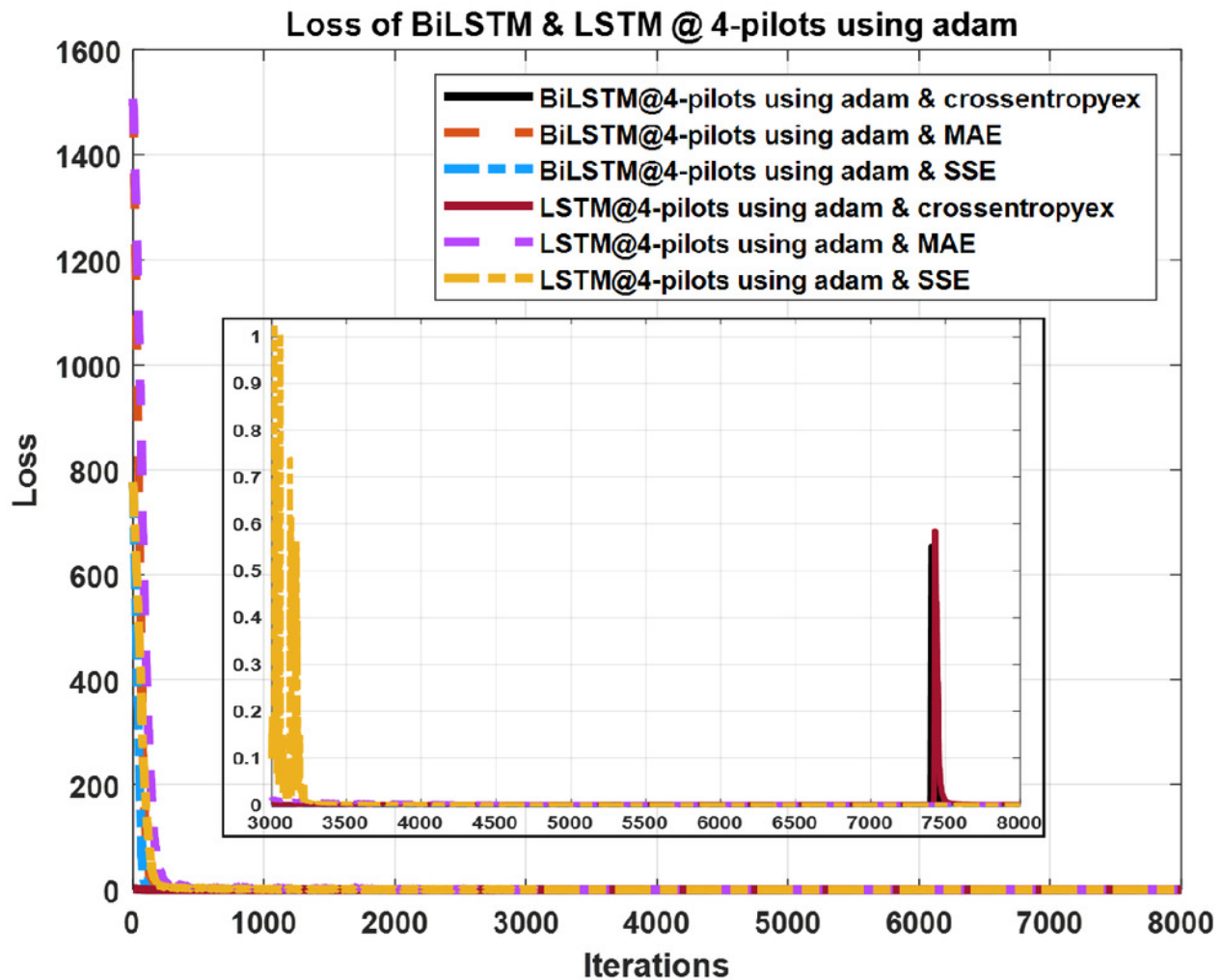


**Table 1** (on next page)

BiLSTM- and LSTM-NN structure parameters and training process options

1  
2  
3  
4  
5  
6  
7  
8

Parameter	Value
Input Size	256
BiLSTM Layer Size	30 hidden neurons
LSTM Layer Size	30 hidden neurons
FC Layer Size	4
Loss Functions	Crossentropyex, MAE, SSE
Mini Batch Size	1000
Epochs Number	1000
Learning Algorithm	Adam
Training Data Size	8000 - OFDM frame
Validation Data Size	2000 - OFDM frame
Test Data Size	10000 - OFDM frame

9  
10  
11  
12  
13  
14  
15  
16  
17  
18  
19  
20  
21  
22  
23  
24  
25  
26  
27  
28  
29  
30  
31  
32  
33  
34

**Table 2** (on next page)

OFDM system and channel parameters

1  
2  
3  
4  
5  
6

<b>Parameter</b>	<b>Value</b>
<b>Modulation Mode</b>	QPSK
<b>Carrier Frequency</b>	2.6 GHz
<b>Paths Number</b>	24
<b>CP Length</b>	16
<b>Subcarrier Number</b>	64
<b>Pilot Number</b>	64, 8 and 4

7  
8  
9  
10  
11  
12  
13  
14  
15  
16  
17  
18  
19  
20  
21  
22  
23  
24  
25  
26  
27  
28  
29  
30  
31  
32  
33  
34  
35  
36

**Table 3** (on next page)

Accuracy comparison of the examined estimators using 64 pilots

1  
2  
3  
4  
5  
6  
7  
8  
9  
10  
11  
12  
13  
14  
15

<b>64 pilots</b>				
	<b>BiLSTM</b>	<b>LSTM</b>	<b>MMSE</b>	<b>LS</b>
<b>Crossentropyx</b>	100	99.99	100	99.94
<b>SSE</b>	99.23	97.88	100	99.96
<b>MAE</b>	99.87	99.52	100	99.97

16  
17  
18  
19  
20  
21  
22

**Table 4**(on next page)

Accuracy comparison of the examined estimators using 8 pilots

1  
2  
3  
4  
5  
6  
7  
8  
9

<b>8 pilots</b>				
	<b>BiLSTM</b>	<b>LSTM</b>	<b>MMSE</b>	<b>LS</b>
<b>Crossentropyx</b>	99.84	99.53	91.34	91.62
<b>SSE</b>	100	99.95	91.60	91.49
<b>MAE</b>	100	99.94	91.53	91.50

10  
11  
12  
13  
14  
15  
16  
17

**Table 5** (on next page)

Accuracy comparison of the examined estimators using 4 pilots

1  
2  
3  
4  
  
5  
6  
7  
8  
9  
10  
11  
12  
13  
14  
15  
16  
17  
18  
19  
20  
21  
22  
23  
24  
25  
26  
27  
28  
29  
30  
31  
32  
33  
34  
35  
36  
37  
38  
39  
40  
41  
42  
43  
44  
45  
46  
47  
48

<b>4 pilots</b>				
	<b>BiLSTM</b>	<b>LSTM</b>	<b>MMSE</b>	<b>LS</b>
<b>Crossentropyex</b>	98.61	97.94	0.24	0.02
<b>SSE</b>	100	99.28	0.24	0.09
<b>MAE</b>	99.97	99.05	0.26	0.04

**Table 6** (on next page)

Processing time comparison of the examined DLNN-based CSIEs

1  
2  
3  
4  
5  
6  
7

	64 pilots		8 pilots		4 pilots	
	Bi-LSTM	LSTM	Bi-LSTM	LSTM	Bi-LSTM	LSTM
Crossentropyex	10:13	8:2	9:14	6:9	8:33	7:53
SSE	10:48	6:57	8:18	7:40	7:43	7:11
MAE	10:43	6:32	9:1	7:24	7:23	7:10

8